J|A|C|S
ARTICLES
Published on Web 01/31/2003

Electrochemical Infrared Characterization of CO Domains on Ruthenium-Decorated Platinum Nanoparticles

Sungho Park,[†] Andrzej Wieckowski,*[,‡] and Michael J. Weaver[†]

Contribution from the Department of Chemistry, Purdue University, West Lafayette, Indiana 47907 and Department of Chemistry, University of Illinois, Urbana, Illinois 61801

Received August 15, 2002; E-mail: andrzej@scs.uiuc.edu

Abstract: Spectra obtained by electrochemical infrared reflection absorption spectroscopy (EC−IRAS) for carbon monoxide (CO) adlayers formed by partial CO dosing on various ruthenium-decorated platinum nanoparticle films are reported. The need to achieve a well distributed rather than aggregated metal nanoparticle array is demonstrated, given that such nanoparticle aggregates induce complex dielectric behavior. The strategy here is to use an "organic glue matrix" (short chain SAMs) between the nanoparticles and the gold substrates. The observed promotion in CO electrooxidation by the existence of a Ru island on Pt nanoparticles, of interest to fuel-cell catalysis, showed a strong relationship with Ru surface concentrations, consistent with previous studies on single crystal or polycrystalline bimetallic surfaces. Two distinctive CO infrared bands, one for the Pt−CO and one for Ru−CO domain were found after the dipole coupling of CO within the two CO domains was minimized. Interestingly, those two CO bands showed independent electrooxidation behavior with electrode potential changes. Also, it is shown that the electrooxidation of CO on large Ru islands is less facile than on small Ru islands. In addition, the activity of commercial Pt/Ru alloy nanoparticles to CO stripping was tested and IRAS spectra were reported as a comparison to our Ru-decorated Pt nanoparticles.

Introduction

Recent years have witnessed a number of impressive examples of nanoparticle-related science, triggered in part by specific applications in catalysis,[1] sensors,[2] spectroscopies,[3] and electrocatalysis.[4,5] Platinum group nanoparticles (especially Pt) constitute interesting electrocatalytic materials which offer high surface area/volume ratios and efficient electrooxidation characteristics, of interest to hydrogen and methanol fuel cells.[4] A fundamental feature of these materials is the ability to alter the average Pt nanoparticle diameter (d) over the range ~2−10 nm, which can yield marked variations in the Pt particle microstructure and, therefore, systematic alterations in their surface properties, which are indeed observed in practice.[6] Given the marked dependence of their electrocatalytic properties on the Pt nanoparticle size, we believe it would be of great interest to explore the catalytic behavior on particles containing deposited metal modifiers, such as Ru, Sn, Bi, and so forth, with which large catalytic effects have been observed on conventional Pt electrodes.[7] Since CO is usually regarded as a catalytic poison or as an oxidation intermediate, the fundamental understanding for electrooxidative promotion of CO on these bimetallic surfaces would be necessary before undertaking an advanced investigation for their electrocatalytic properties toward small organic materials, such as methanol and formic acid.

Examples of studies of CO chemisorbed on a bimetallic structure by infrared absorption spectroscopy (IRAS) with electrode potential control (EC−IRAS),[8,9] in conjunction with other spectroscopies,[10] are numerous. However, there are extremely few corresponding studies on bimetallic nanoparticles, most likely because of the difficulty in immobilization of such

[†] Purdue University.
[‡] University of Illinois.

(1) Kamat, P. V. *J. Phys. Chem. B* **2002**, *106*, 7729.
(2) Mirkin, C. A. *Inorg. Chem.* **2000**, *39*, 2258.
(3) Park, S.; Yang, P.; Corredor, P.; Weaver, M. J. *J. Am. Chem. Soc.* **2002**, *124*, 2428.
(4) For example, see: Carrette, L.; Friedrich, K. A.; Stimming, U. *ChemPhysChem* **2000**, *1*, 162.
(5) (a) Waszczuk, P.; Solla-Gullón, J.; Kim, H.-S.; Tong, Y. Y.; Montiel, V.; Aldaz, A.; Wieckowski, A. *J. Catal.* **2001**, *203*, 1. (b) Chrzanowski, W.; Kim, H.; Wieckowski, A. *Catal. Lett.* **1998**, *50*, 69.
(6) For example, see: McBreen, J.; Mukerjee, S. In *Interfacial Electrochemistry*; Wieckowski, A., Ed.; Marcel Dekker: New York, 1999; p 895.
(7) For example, see: Ross, P. N., Jr. In *Electrocatalysis*; Lipkowski, J., Ross, P. N., Eds.; Wiley-VCH: New York, 1998.
(8) (a) Friedrich, K. A.; Geyzers, K.-P.; Linke, U.; Stimming, U.; Stumper, J. *J. Electroanal. Chem.* **1996**, *402*, 123. (b) Cramm, S.; Friedrich, K. A.; Geyzers, K.-P.; Stimming, U.; Vegel, R.; Fresenius, J. *Anal. Chem.* **1997**, *358*, 189. (c) Kabbabi, A.; Faure, R.; Durand, R.; Beden, B.; Hahn, F.; Leger, J.-M.; Lamy, C. *J. Electroanal. Chem.* **1998**, *444*, 41. (d) Lin, W. F.; Iwasita, T.; Vielstich, W. *J. Phys. Chem. B* **1999**, *103*, 3250. (e) Lin, W. F.; Zei, M. S.; Eiswirth, M.; Ertl, G.; Iwasita, T.; Vielstich, W. *J. Phys. Chem. B* **1999**, *103*, 6968. (f) Iwasita, T.; Hoster, H.; John-Anacker, A.; Lin, W. F.; Vielstich, W. *Langmuir* **2000**, *16*, 522. (g) Liu, R.; Iddir, H.; Fan, Q.; Hou, G.; Bo, A.; Ley, K. L.; Smotkin, E. S.; Sung, Y.-E.; Kim, H.; Thomas, S.; Wieckowski, A. *J. Phys. Chem. B* **2000**, *104*, 3518. (h) Kardash, D.; Korzeniewski, C.; Markovic, N. *J. Electroanal. Chem.* **2001**, *500*, 518.
(9) (a) Gasteiger, H.; Markovic, N.; Ross, P. N., Jr.; Cairns, E. J. *J. Phys. Chem.* **1994**, *98*, 617. (b) Engel, T.; Ertl, G. *Adv. Catal.* **1979**, *28*, 1. (c) Koper, M. T.; Shubina, T. E.; van Santen, R. A. *J. Phys. Chem. B* **2002**, *106*, 686. (d) Massong, H.; Wang, H.; Samjeske, G.; Baltruschat, H. *Electrochim. Acta* **2000**, *46*, 701.
(10) (a) Frelink, T.; Visscher, W.; Cox, A. P.; van Veen, J. A. R. *Ber. Bunsen-Ges. Phys. Chem.* **1996**, *100*, 599. (b) Davies, J. C.; Hayden, B. E.; Pegg, D. J. *Surf. Sci.* **2000**, *467*, 118.

10.1021/ja028154x CCC: $25.00

nanoparticles on conducting substrates, by which enabling electrocatalytic and related spectroscopic analyses. Several surface derivatization schemes along these lines, employing thiol, amine, and other related linkages on glass[11] and gold substrates,[12] have been developed and examined for EC−IRAS suitability.[13]

Armed with the nanoparticle immobilization tactics reported in this paper and information obtained from CO studies on conventional Pt/Ru surfaces, we venture here to examine corresponding electrode potential-dependent spectra for CO irreversibly chemisorbed on various Pt/Ru nanoparticles immobilized by short chain self-assembled monolayers (SAMs) by means of EC−IRAS.

Experimental Section

Platinum/ruthenium nanoparticles were prepared by spontaneous deposition of ruthenium from an aqueous solution of $RuCl_3$ on commercial fuel cell grade platinum black (Pt/black) nanoparticles ($d \approx 6$ nm) purchased from Johnson−Matthey (J−M).[5] The packing density of ruthenium (the ratio of the number of Ru atoms to the number of Pt surface atoms) was estimated by inductively coupled plasma (ICP) spectroscopy and cyclic voltammetry.[5] The average composition of the sample was obtained from ICP, which gave the mass of Pt and Ru in the sample. (The Pt/Ru samples were digested in acid and then diluted for the ICP assay. The final solution typically contained ∼150 ppm of Pt and ∼1 ppm of Ru. The detection limit for Pt and Ru was less than 0.03 ppm for the radial detection. The spectral lines used were 265.945 and 214.423 nm for Pt and 240.272 and 349.894 nm for Ru. Although the concentration of Pt is higher than that of Ru by a factor of ∼150, no interference was observed, since the spectral lines for Pt and Ru are sufficiently separated.) From the mass of Pt, the specific surface area of Pt black, S, the number of surface sites, Γ_{Pt}, and the number of Pt atoms on the surface were calculated, with the knowledge that Ru is only on the surface as two-dimensional islands (see ref 5b for more details). The Ru packing density was then defined as the ratio between the number of Ru atoms on the surface and the number of Pt surface atom, via the formula:

$$\theta_{Ru} = \frac{m_{Ru}}{m_{Pt}} \frac{N_A}{S\Gamma_{Pt}M_{Ru}}$$

where θ_{Ru} is the ruthenium packing density; m_{Ru} and m_{Pt} are the mass of ruthenium and platinum, respectively (from ICP, in grams); N_A is the Avogadro constant; S is the specific surface area of the catalyst, 28 $m^2\ g^{-1}$; Γ_{Pt} is the number of Pt sites per cm^2, 1.3×10^{19} atom m^{-2}; and M_{Ru} is the atomic mass of Ru. Essentially, the monatomic thickness of Ru islands on the Pt support was usually achieved from the present spontaneous deposition.[14] Typically, three samples, having Ru packing densities of 6, 48, and 66%, were prepared by repeating the deposition steps. In addition, the commercial Pt/Ru-50:50(J−M) alloy nanoparticles ($d \approx 2.5$ nm) were purchased from Johnson−Matthey (J−M) and were tested as a reference sample. All the samples will be designated as Pt/Ru-0 (i.e., pure Pt particles), Pt/Ru-6%, Pt/Ru-48%, and Pt/Ru-66%, together with the commercial alloy Pt/Ru-50:50(J−M).

All other chemicals, 3-mercaptopropyltrimethoxysilane (3-MPTS), 3-aminopropyltrimethoxysilane (3-APTMS), and sodium hydroxide (NaOH) were obtained from Aldrich. Supporting electrolytes were prepared from double-distilled H_2SO_4 using ultrapure water from a Millipore Milli-Q system. Electrode potentials were measured and are reported here versus an Ag/AgCl (saturated KCl) reference electrode (Bioanalytical Systems).

Most experimental details of the electrochemical infrared reflection absorption spectroscopy are available elsewhere.[15] As a brief mention, the FTIR spectrometer was a Mattson RS-2 instrument, with a custom-built external reflection compartment containing the narrow-band MCT detector. The metal gold disk substrate, (∼0.9 cm diameter) mounted on a glass plunger by wrapping with Teflon tape, was pressed against the CaF_2 window forming the base of the spectroelectrochemical cell so as to create the optical thin layer.

Results and Discussion

Nanoparticle Immobilization on Gold Substrates. To achieve successfully the goal of interrogating electrochemical and vibrational properties of nanoparticle film, the strategy fulfilling several requirements is necessary.[13] First, the anchored particles should be in electronic "Fermi-level" equilibrium with the substrates, and thereby, their electrode potential can be easily altered, avoiding IR drop interference. Second, the modified surface should retain good reflectivity within the visible and near-IR spectral window to facilitate IRAS analysis. Third, the attachment scheme should not allow aggregation. This last requirement is crucial in interrogating the EC−IRAS data of nanoparticles because of the anomalous "inverted" and/or "bipolar" IRAS bands that can complicate the spectral interpretation.[16,17] The schematic illustration of preparing the appropriate nanoparticle films by the use of short chain SAMs is shown in Figure 1. The polished gold substrates were electrochemically cleaned in 0.05 M H_2SO_4 electrolyte by a few potential cycles between −0.4 and 1.3 V. The substrate was immersed in the 40 mM solution of 3-mercaptopropyltrimethoxysilane (3-MPTS) in methanol for 3 h, thereby producing a SAM.[13,18] After a thorough rinsing with methanol, a 2D-network was induced by dipping the SAM into aqueous 0.01 M NaOH for 2 h, followed by immersing it in the 40 mM solution of 3-aminopropyltrimethoxysilane (3-APTMS) in methanol overnight. The surface, now containing exposed amine moieties, was immersed in a suspension (with stirring) of the desired metal nanoparticles, thus achieving near-monolayer attachment levels. (For more detail analysis, see ref 13.)

Representative EC−IRAS data for saturated CO layers in Pt/black nanoparticle films are displayed in Figure 2. Each absorbance spectrum was obtained at −0.25 V, acquiring 50 interferometer scans, with the solvent and other bulk-phase interferences being removed by subtracting a "reference spectrum" obtained after subsequently stepping to 0.6 V to completely remove the adsorbed CO by electrooxidation.[19] Figure 2 compares spectra in the C−O stretching (ν_{CO}) region for Pt/black nanoparticle films constructed on gold substrates with and without the silane treatment. On the physically immobilized

(11) Freeman, R. G.; Graber, K. C.; Allison, K. J.; Bright, R. M.; Davis, J. A.; Guthrie, A. P.; Hommer, M. B.; Jackson, M. A.; Smith, P. C.; Walter, D. G.; Natan, M. J. *Science* **1995**, *267*, 1629.
(12) (a) Bethell, D.; Brust, M.; Schiffrin, D. J.; Kiely, C. *J. Electroanal. Chem.* **1996**, *409*, 137. (b) Horswell, S. L.; O'Neil, I. A.; Schiffrin, D. J. *J. Phys. Chem. B* **2001**, *105*, 941. (c) Zamborini, F. P.; Hicks, J. F.; Murray, R. W. *J. Am. Chem. Soc.* **2000**, *122*, 4514. (d) Chen, S. *J. Phys. Chem. B* **2000**, *104*, 663. (e) Sagara, T.; Kato, N.; Nakashima, N. *J. Phys. Chem. B* **2002**, *106*, 1205. (f) Liu, Y.; Wang, Y.; Claus, R. O. *Chem. Phys. Lett.* **1998**, *298*, 315. (g) Bharathi, S.; Nogami, M.; Ikeda, S. *Langmuir* **2001**, *17*, 1.
(13) Park, S.; Weaver, M. J. *J. Phys. Chem. B* **2002**, *106*, 8667.
(14) Crown A.; Moraes, I. R.; Wieckowski, A. *J. Electroanal. Chem.* **2001**, *500*, 333.
(15) Chang, S.-C.; Weaver, M. J. *J. Phys. Chem.* **1991**, *95*, 5391.
(16) Park, S.; Tong, Y. Y.; Wieckowski, A.; Weaver, M. J. *Electrochem. Comm.* **2001**, *3*, 509.
(17) Park, S.; Tong, Y. Y.; Wieckowski, A.; Weaver, M. J. *Langmuir* **2002**, *18*, 3233.
(18) (a) Robertson, J. W.; Cai, M.; Pemberton, J. E. *Adv. Mater.* **2001**, *13*, 662. (b) Cai, M.; Ho, M.; Pemberton, J. E. *Langmuir* **2000**, *16*, 3446.
(19) Chang, S.-C.; Weaver, M. J. *J. Chem. Phys.* **1990**, *92*, 4582.

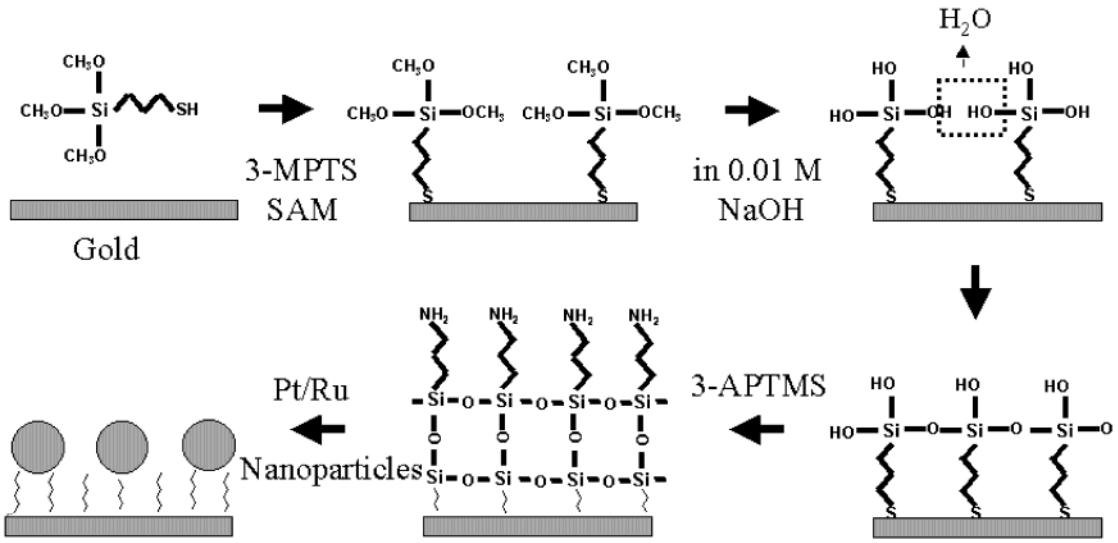

Figure 1. Schematic steps involved in preparing the nanoparticle films. (See text.)

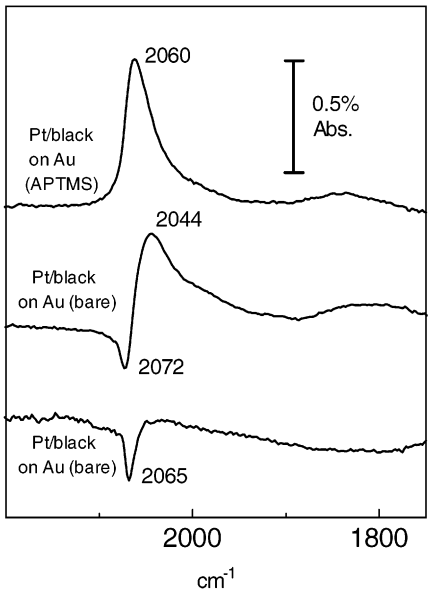

Figure 2. Comparison of IRAS spectra for saturated CO adlayers on Pt/black nanoparticle ($d \approx 6$ nm) films, prepared by using APTMS film, and physically anchored on bare Au substrates, as indicated, at −0.25 V vs Ag/AgCl in 0.05 M H_2SO_4.

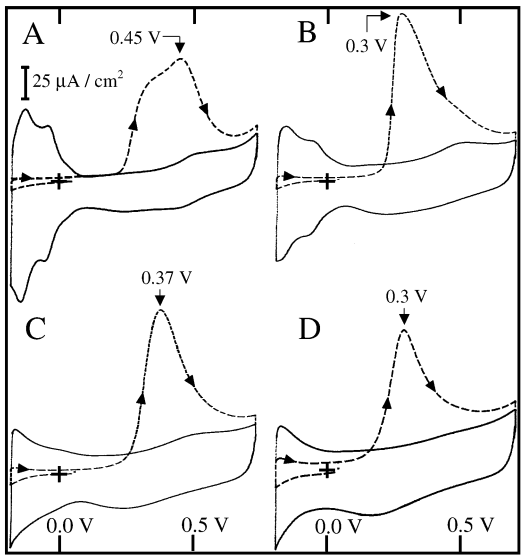

Figure 3. Comparison of illustrative voltammograms (50 mV s^{-1}, vs Ag/AgCl) on (A) Pt/Ru-6%, (B) Pt/Ru-48%, (C) Pt/Ru-66%, and (D) Pt/Ru-50:50(J−M) attached on Au as in Figure 1, without (solid trace) and with (dashed trace) saturated CO adlayers, in 0.05 M H_2SO_4. (The current density scales refer to the geometric area of the planar gold substrates.)

Pt/black nanoparticle films, immediately noticeable is the presence of a "dip" at 2072 cm^{-1} in the absorbance baseline at slightly higher frequencies than in the case of the positive-going band peak. This negative-going component becomes progressively more pronounced for thicker films and, in some cases, even shows inverted unipolar behavior, as exemplified by the bottom spectrum. Obviously, bipolar and/or inverted bands complicate the data analysis. Although this feature, which is apparently associated with the anomalous dielectric properties of the aggregated metal nanoparticles,[20] can be minimized by the use of physically deposited ultrathin (1−2 equivalent monolayer) films,[16,21] the absolute control of this band abnormality can be achieved only by the well distributed metal nanoparticle array.[13] We could then examine corresponding electrode potential-dependent spectra for CO chemisorbed on ruthenium-decorated Pt/black nanoparticles, as reported later.

Cyclic Voltammetry. Typical voltammograms for various Pt/Ru nanoparticles, anchored on polished gold substrates via the procedure mentioned previously, are shown as the solid trace in Figure 3, acquired (at 50 mV s^{-1}) from −0.2 to 0.75 V versus Ag/AgCl in 0.05 M H_2SO_4, featuring the well-known hydrogen adsorption/desorption profile below 0 V, characteristic of Pt electrodes. There are obvious changes in the CV morphology with different Pt−Ru compositions. As the amounts of Ru increase, the peak for "hydrogen underpotential deposition (upd)" is attenuated markedly, with the increase of the charge in the double-layer region. These features are in good agreement with those observed previously on Ru-modified Pt(111) electrodes and nanoparticle systems.[5,8e] As noticed by Gasteiger et

(20) (a) Bjerke, A. E.; Griffiths, R. R.; Theiss, W. *Anal. Chem.* **1999**, *71*, 1967. (b) Lu, G.-Q.; Sun, S.-G.; Chen, S.-P.; Cai, L.-R. *J. Electroanal Chem.* **1997**, *421*, 19. (c) Zhu, Y.; Uchida, H.; Watanabe, M. *Langmuir* **1999**, *15*, 8757. (d) Ortiz, R.; Cuesta, A.; Marquez, O. P.; Marquez, J.; Mendez, J. A.; Gutierrez, C. *J. Electroanal. Chem.* **1999**, *465*, 239.

(21) Park, S.; Wasileski, S.; Weaver, M. J. *J. Phys. Chem. B* **2001**, *105*, 9719.

al., it indicates the formation of oxygen-like species on the surface at more negative potentials.[22] This plays an important role in progressively lowering the potential of irreversible CO electrooxidation (dashed trace). The corresponding dashed traces in Figure 3 were obtained following a saturated dosage of CO, by bubbling in CO gas and then following by argon purging. The slight modification of the Pt/black surface with Ru (~6%) brought a significant change in the CO stripping peak (Figure 3A). A pure Pt/black nanoparticle film shows a CO stripping peak at 0.45 V with a narrower peak width (which is not shown here).[13] The broad CO stripping peak on Pt/Ru-6% is due to the overlap of two CO peaks, consistent with the observations on a single crystal Pt(111)/Ru[9d] and on Pt/Ru nanoparticles.[23] The further Ru decoration (Pt/Ru-48%) lowers the CO stripping peak potential down to 0.3 V, together with that of the small shoulder around 0.45 V. However, increasing the surface Ru concentration up to 66% shows slightly increased CO stripping peak potentials around 0.37 V. It was reported that the maximum activity toward CO oxidation could be achieved by an Ru surface composition of 50%, since it maximizes the number of Pt−Ru neighbors and hence provides more nucleation sites.[9a] The CO oxidation on Pt/Ru nanoparticles shows very similar trends as on poly/single crystalline Pt/Ru alloy surfaces. In both cases, Ru sites near Pt atoms nucleate oxygen-containing species at low electrode potentials and, thereby, lower the onset potential of CO oxidation.

Also, it was suggested that OH_{ads}, the most likely form of oxygen-containing species in the electrochemical system, would make a stronger adsorption depending on the nature of atoms comprising the surface ensembles.[9a] The suggested dependence of adsorption strength of OH_{ads} on multiple Ru sites seems to play a role in the irreversible CO electrooxidation on Ru-decorated Pt nanoparticle films. Since we are changing the Ru ensemble size by repeating the spontaneous Ru deposition steps on Pt nanoparticles, the insight into this assumption can be obtained from EC−IRAS experiments, as will be described later. The commercial Pt/Ru alloy nanoparticle films show the CO oxidation peak at 0.3 V (Figure 3D), which is similar to that of Pt/Ru-48% except for the less defined hydrogen adsorption/desorption peaks.

Nanoparticle Surface Composition-Dependent CO EC−IRAS Spectra. Of central interest here is the detailed nature of the ν_{CO} absorbance spectra for the Pt/Ru nanoparticle film electrodes as a function of Pt/Ru surface compositions. Representative spectra obtained for CO saturated layers for four different Ru surface concentrations on Pt nanoparticles [Pt/Ru-6%, -48%, -66%, and -50:50(J−M) alloy], at −0.25 and 0.00 V versus Ag/AgCl, are shown in Figure 4A and B, respectively. The band, which is assigned to atop CO coordination, appears at ~2060 cm^{-1}, together with a weak and broad feature of the bridging CO centered at ~1850 cm^{-1}.[24] Very similar band shapes were obtained over the potential range −0.25 to 0.1 V prior to the onset of CO electrooxidation. The dependence of the peak ν_{CO} frequency (ν^{P}_{CO}) on the potential (E) (the so-called Stark-tuning rate, $d\nu^{P}_{CO}/dE$), typically around 25−35 cm^{-1} V^{-1}, is essentially close to the values obtained for

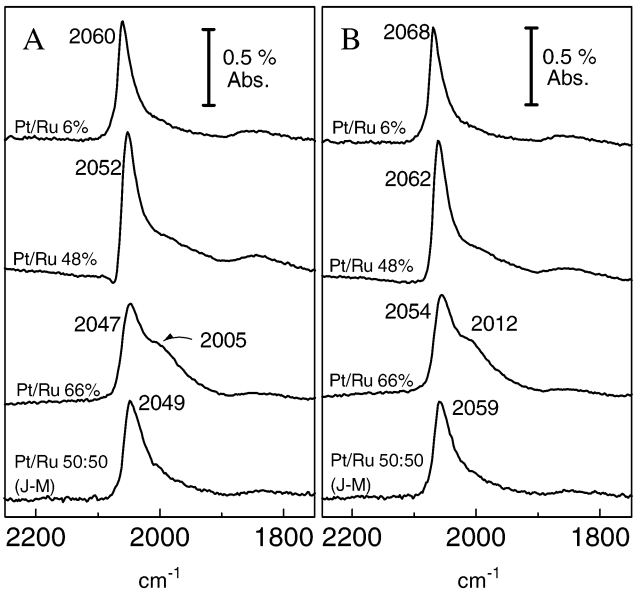

Figure 4. Selected infrared absorbance spectra (A) at −0.25 V and (B) at 0.0 V vs Ag/AgCl in 0.05 M H_2SO_4 for saturated CO packing densities ($X_{CO} = 1$) on various Pt/Ru nanoparticles, as indicated.

conventional Pt electrodes and various sizes of carbon-supported Pt nanoparticles.[21] Careful inspection of the spectral data in Figure 4A reveals several crucial features. Most obviously, the ν^{P}_{CO} value at a given potential, −0.25 V, is seen to be red shifted compared with the value (~2070 cm^{-1}) on the conventional polycrystalline Pt (Pt/poly). (The CO spectrum on Pt/Ru-0% is essentially the same as that obtained on Pt/Ru-6%; see Figure 2.)

This red shift, discussed in detail in ref 21, has been ascribed primarily to a systematic diminution of the average surface coordination number (*cn*) with decreasing particle size. The size-dependent *cn* transition from the terrace sites ($cn = 9$) to the edge and vertex ($cn \approx 6-7$ or even lower) is expected on the basis of an ideal icosahedral/cuboctahedral and related metal packing arrangement where the particles assume pseudo-spherical shapes.[21,25] There are X-ray absorption study evidences[6,26c] which also show the increased Pt−OH and Pt−CO binding energies on the smaller nanoparticles, in good agreement with the expected increasing dominance of edge/vertex sites. Thus, the red shifted CO frequency reflects an increasing $d\pi-2\pi^*$ back donation yielding stronger metal−CO binding for Pt nanoparticles with smaller *cn* values compared with those of Pt/poly. Another essential feature in Figure 4 is the progressive augment of shoulder around ~2005 cm^{-1} as the surface Ru concentration increases. Obviously, this band can be assigned to atop CO on the Ru islands. It is worthy of mention that this is the first observation of two CO vibrational bands on nanoscale bimetallic Pt/Ru electrodes, even though the similar features were previously observed on a surface made of electrochemically deposited Ru on Pt(111).[8b,d] The vibrational features, however, are not as distinctive as were those on single crystal Pt(111)/Ru. The ν_{CO} band shapes on nanoparticles usually show a long "tail" toward lower wavenumbers.[21] This profile, which

(22) Gasteiger, H. A.; Markovic, N.; Ross, P. N., Jr.; Cairns, E. J. *J. Phys. Chem.* **1993**, *97*, 12020.
(23) Tong, Y. Y.; Kim, H. S.; Babu, P. K.; Waszczuk, P.; Wieckowski, A.; Oldfield, E. *J. Am. Chem. Soc.* **2002**, *124*, 468.
(24) Villegas, I.; Weaver, M. J. *J. Chem. Phys.* **1994**, *101*, 1648.
(25) Park, S.; Wasileski, S. A.; Weaver, M. J. *Electrochim. Acta* **2002**, *47*, 3611.
(26) (a) Frelink, T.; Visscher, W.; van Veen, J. A. R. *J. Electroanal. Chem.* **1995**, *382*, 65. (b) He, C.; Kunz, H. R.; Fenton, J. M. *J. Electrochem. Soc.* **1997**, *144*, 970. (c) Mukerjie, S.; McBreen, J. *J. Electroanal. Chem.* **1998**, *448*, 163.

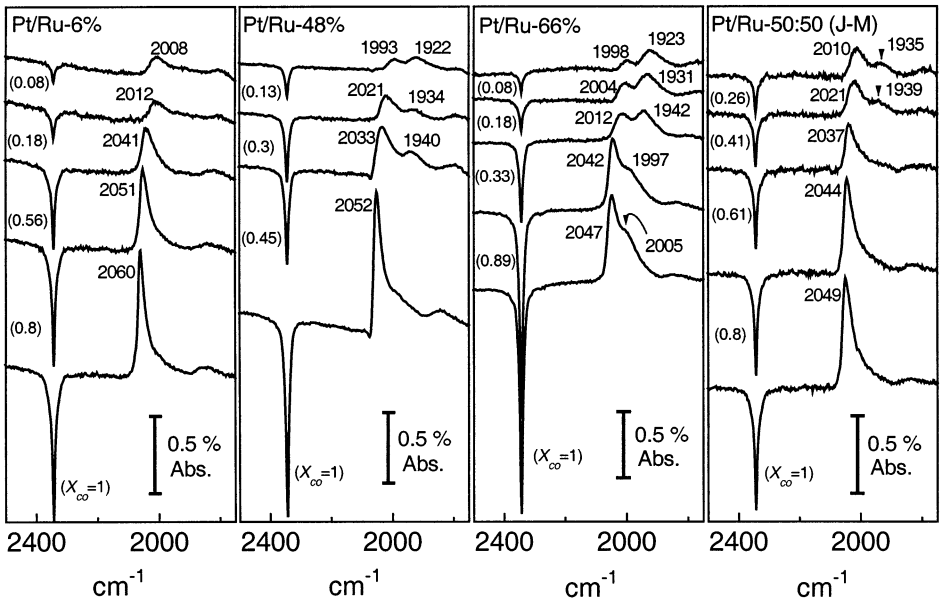

Figure 5. Selected IRAS spectra for different subsaturated CO packing densities (X_{CO}, as indicated in parentheses) for various Pt/Ru nanoparticles, as denoted, at −0.25 V vs Ag/AgCl in 0.05 M H_2SO_4.

is not seen on conventional Pt/poly, has been ascribed partly to nanoparticle polydispersity.[21] The broad bandwidth, together with a long tail, makes it hard to observe the CO bands on Ru domains with the slight Ru decoration (∼6%) on Pt nanoparticles. Apparently, a sufficiently large Ru domain (∼48 or 66%) is required to make such observations. However, the CO band intensity on Pt islands is much greater than that for the lower frequency component on the Ru islands. A simple picture of the dipole−dipole coupling, inducing the "intensity transfer" from the lower- to the higher-frequency components, can explain the mismatch between the CO band intensity and the surface composition.[27] As shown from the comparison study of the experimental ν_{CO} data with the theoretically simulated spectra,[28] the "CO dynamic dipole−dipole coupling" between the Pt and Ru regions plays an important role in enhancing the former band intensity. Notably, if the Pt/Ru alloy surfaces were atomically intermixed, the spectra would exhibit a single ν_{CO} band (for saturated CO adlayers) having a similar form to those obtained on the pure polycrystalline metals.[19] For Pt/Ru-50:50(J−M), however, there is also a weak shoulder around 2035−2039 cm^{-1}, showing the presence of low-density ruthenium islands on the homogeneous alloy surface. Also evident in Figure 4 is the progressive red shift of ν^{p}_{CO} on Pt sites with the increase in Ru surface concentration.

If the real CO coverage for each sample is different with the surface composition variation, it will bring the red shift of the C−O stretching band due to diminution of the dipole coupling. However, CO adsorption energies on various crystal planes of Pt and Ru are similar within 15%.[9b] While density functional theory (DFT) calculations showed a difference (0.32 eV) in bonding energies of CO between Pt(111) and Ru(0001) surfaces,[9c] the calculations also showed a higher bonding energy of CO on Ru than that on Pt. Thus, the Ru presence would not bring a CO coverage decrease because of higher CO affinity toward the Ru domains. Furthermore, the CO stripping charges on those different nanoparticle films, as evident in Figure 3, are more or less similar, which is consistent with the previously reported results.[23] Thereby, the explanation for coverage-dependent red shift is not plausible in this case. The other possible suggestion is the alteration of the electronic nature of Pt by neighbor Ru atoms. Lin et al. found that CO bound to the Ru (75%)-modified Pt(111) displayed a stretching frequency that is ∼10 cm^{-1} lower than that on pure Pt(111) and suggested a significant electron transfer from the Ru to adjacent Pt atoms, driven by the work function difference between Ru (4.71 eV) and Pt(111) (5.39 eV).[8d] Such an electronic effect should induce the increasing $d\pi-2\pi^*$ back donation on Pt islands, reflected by the ν_{CO} red shift. This suggestion is also supported by our present results. However, we do not think the electronic modification is mainly responsible for CO electrooxidation promotion, since the same ν_{CO} red shift that was observed in pure Pt nanoparticle systems with size variations did not show any benefit in terms of CO electrooxidation.[16,21] Moreover, there is another very recent study clearly demonstrating only the surface Ru is responsible for promoting CO electrooxidation, assisted by the surface composition information obtained from various techniques, such as low energy ion scattering spectroscopy (LEISS), X-ray photoelectron spectroscopy (ARXPS), low energy electron diffraction (LEED),[10b] and EC NMR.[23] It was found that no promotion was observed when Ru is excluded from the top layer, but substantial concentrations are present in the second and third layers.[10b]

Further insight into the comparative vibrational CO features on these materials can be obtained by minimizing the dipole−dipole coupling, since it obscures, in the present bimetallic nanoparticle system, the distinct observation and/or analysis of CO behavior on Pt and Ru islands. A tactic that has proven valuable, experimentally[29] and theoretically,[30] for minimizing the coupling effect involves obtaining coverage-dependent infrared spectra. Figure 5 shows typical spectra obtained at

(27) (a) Hollins, P.; Pritchard, J. *Prog. Surf. Sci*. **1985**, *19*, 275. (b) Hoffmann, F. M. *Surf. Sci. Rep.* **1983**, *3*, 107. (c) Ueba, H. *Surf. Sci.* **1987**, *188*, 421. (d) Hollins, P. *Surf. Sci. Rep.* **1992**, *16*, 51.
(28) Zou, S.; Villegas, I.; Stuhlmann, C.; Weaver, M. J. *Electrochim. Acta* **1998**, *43*, 2811.
(29) Chang, S.-C.; Weaver, M. J. *J. Chem. Phys*. **1990**, *92*, 4582.
(30) Severson, M. W.; Weaver, M. J. *Langmuir* **1998**, *14*, 5603.

−0.25 V for a range of submonolayer CO adlayers formed on various Pt/Ru nanoparticle films. The adsorption electrode potential was selected within the so-called "hydrogen" region where the primary coadsorbed species is hydrogen. It was found that smaller and more coverage-dependent CO patches resulted from CO dosing in the electrochemical hydrogen region.[29] In other words, more well distributed CO adlayers (at low coverages) can be achieved in the presence of hydrogen relative to the "double-layer" potential window where water is the main coadsorbed species, partly because of the more effective adsorption competition of hydrogen compared with water. The lower coverages were acquired by dosing with diluted ($\sim 10^{-5}$ M) CO solutions for controlled times, typically <2 min. (The same tactic is used to generate lower CO coverages on planar Pt electrodes.[29]) Each spectrum shown was obtained by 50 interferometer scans at −0.25 V and subsequently subtracting the reference spectrum acquired at 0.6 V from each set. The fractional CO coverages, X_{CO}, were attained from the absorbance of the 2345 cm^{-1} band due to CO_2 trapped within the thin layer, relative to the value for a saturated adlayer ($X_{CO} = 1$). The ν_{CO}^{P} frequencies for Pt/Ru-6% at low X_{CO} are seen to be substantially red shifted (by ~60 cm^{-1}). The extent of these red shifts is markedly beyond that (20−30 cm^{-1}) expected on the basis of the diminishing dipole coupling induced by coverage changes, as observed on structurally uniform low-index single crystal surfaces such as Pt(111).[29]

Most likely, this observation, consistent with that on carbon-supported pure Pt nanoparticles,[21] reflects in part the preferential adsorption of CO to edge and other low-coordination Pt sites at lower X_{CO} because of the higher binding energies compared with the case of terrace sites.[31] It is well-known that CO bound to low-coordination sites such as edges and vertexes yields red shifted ν_{CO}^{P} values relative to those of terrace binding.[21,32] Furthermore, the red shifted tail "envelope" (in the range, ~2060−1900 cm^{-1}) of the saturated adlayer ($X_{CO} = 1$) spectrum suggests that such a distribution of coordination sites is primarily responsible for the remarkable ν_{CO}^{P} red shift.

As expected from the dipole coupling considerations, the minimized "dipole coupling" between Pt and Ru islands should enable the observation of two distinctive CO bands, evident clearly in Figure 5. The highly Ru decorated Pt nanoparticles (~48%) exhibit the CO band on Ru sites around ~1934 cm^{-1} at the given low coverage ($X_{CO} \approx 0.3$), separated from the atop and bridging CO bands at ~2021 and 1850 cm^{-1}, respectively. Also, of typical interest are the roughly proportional band intensities from each domain to surface metal concentrations. This feature is more pronounced on Pt/Ru-66%, as demonstrated by the slightly higher band intensity at 1942 cm^{-1} on Ru relative to Pt domains (at 2012 cm^{-1}). It confirms again the lessened "dipole coupling" to a great extent, resulting in the diminution of "intensity transfer" from the lower- (such as Ru-bound CO) to the higher-frequency (i.e., Pt-bound CO) oscillators, thereby representing more or less the surface metal island concentrations. The same experiment with commercial Pt/Ru-50:50(J−M) alloy nanoparticles reveals the existence of segregated Pt and Ru domains to some extent, illustrated evidently by two CO bands centered at 2010 and 1935 cm^{-1}, respectively, at low CO coverage ($X_{CO} \approx 0.26$).

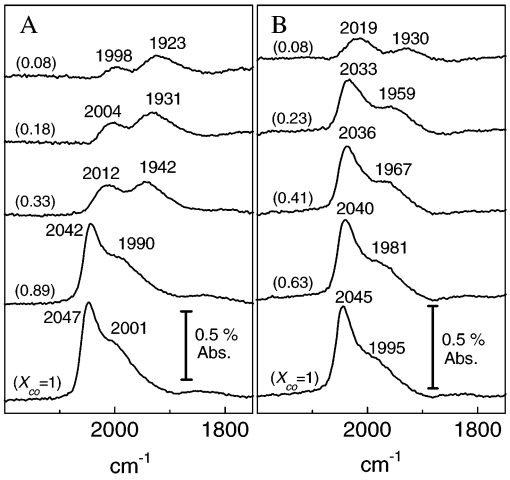

Figure 6. Representative IRAS spectra in the ν_{CO} region 1750−2200 cm^{-1} for various subsaturated CO packing densities (X_{CO}, as indicated in parentheses) obtained on Pt/Ru-66%, by (A) "dosing" for various times from dilute CO solutions and by (B) progressive electrooxidative "stripping" from a saturated CO adlayer ($X_{CO} = 1$), at −0.25 V vs Ag/AgCl in 0.05 M H_2SO_4.

An issue of essential significance involves the dependence of the CO adlayer structure upon the factional adsorbate coverage X_{CO}. A means utilized in characterizing adsorbate interactions in a ultrahigh vacuum (UHV) system concerns obtaining coverage-dependent infrared spectra for various portions of isotopic mixtures, such as $^{12}CO/^{13}CO$.[27a,b] This tactic, separating adsorbate−adsorbate interactions $\Delta\nu$ into individual components associated with "dynamic" dipole−dipole coupling $\Delta\nu_D$ and "static" dipole and chemical contributions $\Delta\nu_C$,[27a,b] also provided a means of exploring the effects of the double-layer environment on the coverage-dependent structure of electrochemical adsorbates.[29] So far, however (to our knowledge), this tactic has been restricted to monometallic surfaces. The bimetallic systems, such as our Pt/Ru nanoparticles, would not provide valuable information (in terms of band intensities) by the same type of isotopic mixture experiment, since the ν_{CO} frequencies of ^{13}CO on Pt sites (as expected from the carbon mass change) downshift by 45−50 cm^{-1} and hence overlap with the ν_{CO} band of ^{12}CO on Ru domains. Also, there is still considerable "intensity transfer" from the lower- to the higher-frequency band component in 1:1 $^{12}CO/^{13}CO$ mixtures, observed previously in both the electrochemical[29] and UHV[33] systems on pure Pt(111). However, another critical insight into CO adlayer structure at subsaturated coverages can be obtained from comparison of Figure 6 A and B, containing representative absorbance spectra at −0.25 V at the various coverages. The left-hand set of spectra (Figure 6A), as described previously, was obtained by employing various dosing times of a lower CO solution concentration (~10^{-5} M) to the Pt/Ru-66% nanoparticle films at −0.25 V. In contrast, the right-hand set of spectra (Figure 6B) was acquired by starting with a saturated CO adlayer on the same material, formed by CO gas bubbling for a few minutes and then purging with argon to remove the dissolved CO. Each spectrum shown was attained at −0.25 V, repeating the potential stepping up to 0.6 V for ~2 s and then down back to −0.25 V between each set so as to electrooxidize

(31) Hammer, B.; Nielson, O. H.; Norskov, J. K. *Catal. Lett.* **1997**, *46*, 31.
(32) Brandt, R. K.; Hughes, M. R.; Bowget, L. P.; Truszkowski, K.; Greenler, R. G. *Surf. Sci.* **1993**, *286*, 15.
(33) (a) Olsen, C. W.; Masel, R. I. *Surf. Sci.* **1988**, 201, 444. (b) Olsen, C. W.; Masel, R. I. *J. Vac. Sci. Technol., A* **1988**, *6*, 792.

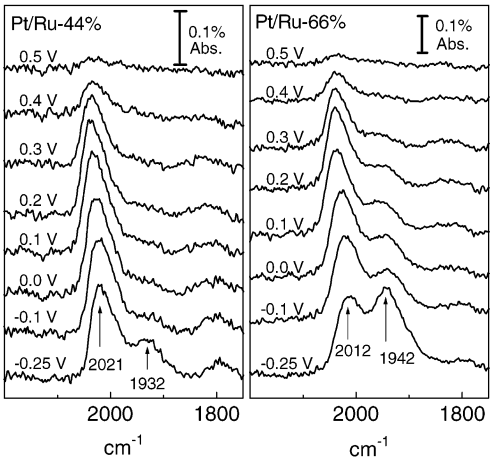

Figure 7. Comparison of typical EC−IRAS spectra for the subsaturated ($X_{CO} \approx 0.3$) CO adlayer on Pt/Ru-48% and on Pt/Ru-66%, as indicated, vs Ag/AgCl in 0.05 M H_2SO_4.

a fraction of the adsorbed CO each time. The reference spectrum was obtained after the complete oxidation, as usual to eliminate other solvent interferences. The intermediate coverage estimation was made from the absorbance of the solution CO_2 band at 2345 cm^{-1} (vide supra). Comparison of the data in Figure 6A and B exhibits remarkable differences in the coverage-dependent ν_{CO} band spectra under such CO "dosing" and "stripping" conditions. CO "dosing" yields the peak frequency ν^{P}_{CO} band on Pt sites decreased significantly by about 50 cm^{-1}, from ~2047 to 1998 cm^{-1}, over the X_{CO} range from 1 to 0.08, because of diminution of the degree of dipole coupling to a great extent toward lower coverages.

As already mentioned above, ν_{CO} band intensities from each domain (Pt and Ru sites) are proportional to the surface metal island concentrations under the minimized dipole coupling conditions. (The reliable relative surface metal island concentrations can be roughly estimated by each ν_{CO} band intensity at $X_{CO} \approx 0.3$ now that the band intensities are strong enough to be calculated with greatly minimized dipole coupling.) In strong contrast, the corresponding ν^{P}_{CO} band obtained under electrooxidatively "stripping" conditions decreases by only about 25 cm^{-1}, to 2019 cm^{-1} at $X_{CO} \approx 0.08$, as shown in Figure 6B, indicating that extensive CO island formation survives to lower CO coverages. Significantly, no noticeable changes in the band intensity ratio between ν_{CO} on Pt and Ru islands are observed over the entire X_{CO} range during adlayer electrooxidation, suggesting again that the microscopic CO adlayer structure remains mostly intact and hence the extent of the dipole coupling is largely maintained even down to low X_{CO} values (~0.08).

Spectral Behavior of CO on Ru and Pt Islands. Of essential importance here is the comparison of potential-dependent ν_{CO} data obtained on various Pt−Ru nanoparticles with different surface compositions. Given that the dipole coupling plays an important role in the form of IRAS ν_{CO} band shapes and intensities, we find it is appropriate to examine ν_{CO} absorbance spectra attained at low CO coverages, however, with reliable intensities from each component (vide supra). Figure 7 shows the representative potential-dependent CO spectra acquired for Pt/Ru-48% and Pt/Ru-66%, respectively, for low "dosing" CO coverage ($X_{CO} \approx 0.3$). Clearly, the ν_{CO} band changes with surface potential alterations. The spectra produced on Pt/Ru-48% display two individual CO bands: one from Pt and the other from Ru sites, centered at ~2021 cm^{-1} and 1932 cm^{-1}, respectively. The band from Ru sites starts to *first* disappear immediately after the surface potential was stepped upward to −0.1 V while retaining the intensity and shape of the corresponding band on Pt sites. The band on Ru can be hardly detected at 0.2 V, with no noticeable change in ν_{CO} band intensity on Pt. Significantly, those two individual bands display independent behavior reflecting first electrooxidation of CO on Ru sites and then on Pt sites, consistent with previous results on Pt(111)/Ru surfaces.[35] This feature, as shown in the right-hand data set, is more pronounced on the more Ru rich Pt nanoparticles (Pt/Ru-66%). The spectra obtained from Pt/Ru-66% exhibit a more intense ν_{CO} band on the Ru island, consistent with the surface metal compositions than is the case from Pt/Ru-48%. The other feature seen in the right-hand data set, the survival of the intense band appearing at ~1942 cm^{-1} (on Ru sites) up to a significantly higher potential (~0.2 V) with reduced intensities, signals the endurance of CO on Ru sites at this potential. In addition, once again, the ν_{CO} band on Pt sites is preserved without intensity changes, except for the peak frequency shifts (normal Stark-tuning effects). The obvious difference between Pt/Ru-48% and Pt/Ru-66% is the multiple Ru−Ru ensemble size. At a given and relatively low CO fractional coverage, for example, $X_{CO} \approx 0.3$, minimizing the dipole coupling complication occurs to a great extent, and the individual ν_{CO} band intensities are proportional to the surface metal ensemble size. As evident in the right-hand segment in Figure 7, progressively decreasing the ν_{CO} band intensities on Ru sites with a potential upward stepping, nonetheless, still surviving up to ~0.2 V, represents the slower CO (on Ru domains) electrooxidation for Pt/Ru-66%, relative to the Pt/Ru-48% nanoparticle films. This simply demonstrates that the Pt/Ru-66% film has fewer reactive sites than the Pt/Ru-48 surface.

Now, after being given such rich information relating electrochemical ν_{CO} spectra with surface compositions and particle size at subsaturated CO coverages to minimize obscuring dipole coupling, we can analyze potential-dependent ν_{CO} spectra at CO saturated coverages ($X_{CO} = 1$). Figure 8 shows typical CO saturated adlayer ν_{CO} spectra obtained on Pt/Ru-6%, /Ru-48%, and /Ru-66%, respectively. As exemplified earlier in Figure 4, the ν_{CO} band shapes are invariant over the potential range −0.25 to 0.1 V prior to the onset of CO electrooxidation. Thereby, for data clarity, only two ν_{CO} bands are shown for each sample at −0.25 (solid trace) and 0.2 V (dashed trace). Careful inspection of Figure 8 reveals several important features. On the Pt/Ru-6% nanoparticle films, closely similar ν_{CO} band shapes were obtained at −0.25 and 0.2 V, except for the usual ν_{CO} frequency−E (Stark-tuning) shift. Nevertheless, significantly different ν_{CO} band shapes were attained at the given potentials on the Pt/Ru-48% film, including no ν_{CO} band frequency shift. The ν_{CO} band component on Pt domains, as clearly shown in Figure 7, should not decrease at this potential (0.2 V). The CO saturated adlayers usually undergo slightly less facile electrooxidation than well distributed small CO patches (like the case in Figure 7), since CO electrooxidation occurs via nucle-

(34) Lu, C.; Rice, C.; Masel, R. I.; Babu, P. K.; Waszczuk, P.; Kim, H. S.; Oldfield, E.; Wieckowski, A. *J. Phys. Chem. B* **2002**, *106*, 9581.
(35) Lu, G.-Q.; Waszczuk, P.; Wieckowski, A. *J. Electroanal. Chem.* **2002**, *532*, 49.

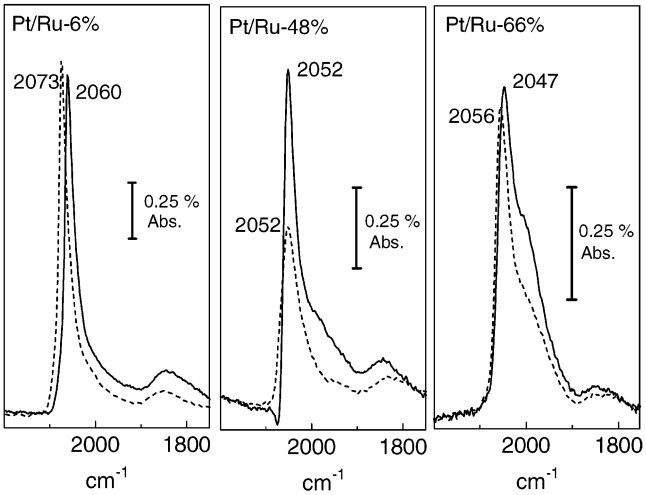

Figure 8. Comparison of representative EC−IRAS spectra for the saturated CO adlayer on various nanoparticle films, as indicated, at −0.25 (solid trace) and at 0.2 V (dashed trace) vs Ag/AgCl in 0.05 M H_2SO_4.

ation and growth at the edge of CO islands.[30] Thereby, the significant decrease of the ν_{CO} band intensity on Pt domains (centered at 2052 cm^{-1}) concomitant with the noticeable damping of the corresponding ν_{CO} band component on Ru sites (around 2000 cm^{-1}) is induced by the almost complete CO electrooxidation *only* on Ru islands (see Figure 8, the middle set).

After CO oxidation on Ru sites, the loss of "dipole coupling" between CO on Pt and Ru leads to the decrease of ν_{CO} band intensity (at 2052 cm^{-1}) and no shift of the ν_{CO} band frequency with surface potential increase, as the usual ν_{CO} frequency−E (Stark-tuning) shift is traded off by the disappearance of the dipole coupling contribution from CO on Ru sites. Previously, Lin et al. reported that FTIR spectra for CO saturated adlayers on a Ru-modified Pt(111) electrode with various Ru coverages showed the decrease of the band intensities of CO on Ru and on Pt simultaneously and made a conclusion that the electrooxidation of CO on Ru and on Pt starts at the same potential.[8d] *However, with dipole coupling considerations at CO saturation coverages, our present study shows that the individual ν_{CO} band components from Pt and Ru domains behave independently with surface potential variations, as evident in Figure 7 at submonolayer coverages.* In harmony with the potential-dependent ν_{CO} data at low CO coverages (Figure 7, the right-hand set), the CO saturated adlayers on Pt/Ru-66% shows the survival of the ν_{CO} band component on Ru sites (around 2000 cm^{-1}) to a significant extent, together with the only slight decrease of ν_{CO} band intensity on Pt islands, representing the existence of "dipole coupling" still at this potential, 0.2 V. (Figure 8, the far right-hand data.)

A further insight into the CO electrocatalytic oxidation dependence on Ru surface concentration can be obtained from the inspection of potential-dependent CO_2 bands, which is shown in Figure 9. The onset electrode potentials of CO oxidation depend on surface Ru concentrations. As shown in the previous figures, the Pt/Ru-48% and the Pt/Ru-66% films illustrate very comparable CO_2 onset potentials. (Please note 0.1 V lower onset potentials for Pt/Ru-48 or -66% than for Pt/Ru-6% samples.) Also, the CO_2 peak area ratios at 0.2 V (compared to its complete oxidation peak area at higher potentials, ∼0.6 V) representing the relative catalytic activities at low potentials illustrate that Pt/Ru-48% is a better catalyst than Pt/Ru-66%, consistent with the analysis obtained from CO region in Figure 8. On the basis of CV and IRAS experiments, it shows the order of catalytic activities for CO oxidation at 0.2 V: Pt/Ru-48% > Pt/Ru-66% > Pt/Ru-6%.

These results show that CO adsorbed on the Ru sites at the Pt−Ru boundaries oxidizes first with the electrode potential increases, since those sites facilitate the nucleation of oxygen-containing species. At lower potentials, Pt sites are less reactive than Ru, because the OH on Pt is not yet formed.[35] However, if the Ru−Ru ensemble size increases more (like our Pt/Ru-66% sample), the CO on the Ru sites far from the Pt−Ru boundaries does not readily oxidize because of the intrinsically low CO oxidation rate constant of Ru domains.

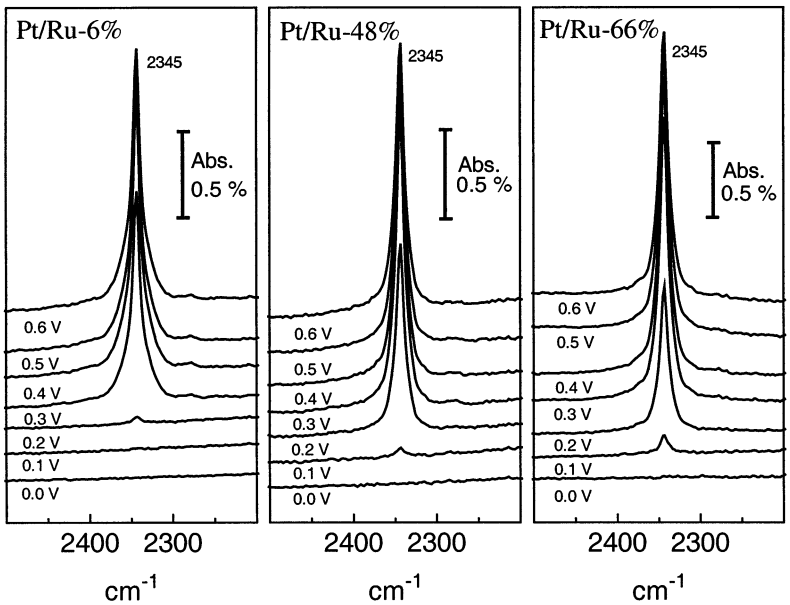

Figure 9. Representative EC−IRAS spectra for the potential-dependent CO_2 bands on three different nanoparticle films in 0.05 M H_2SO_4. Potentials are quoted vs Ag/AgCl. The reference spectrum was obtained at −0.25 V. The coverage is the saturation coverage.

Concluding Remarks

Overall, the present results demonstrate clearly that EC−IRAS can provide a powerful analytical means for scrutinizing in situ characteristics of adsorbates on mono- or bimetallic nanoparticle systems. Given that Pt group nanoparticles are key materials in hydrogen and methanol − air fuel cells, we find it surprising that there are very scarce reports regarding EC−IRAS with Pt group nanoparticles compared with single crystalline or polycrystalline surfaces. It is mainly due to the difficulty in preparing monolayer-level films of metal nanoparticles exhibiting near-ideal IRAS as well as electrochemical properties. The present study, utilizing for the first time the chemical modification to anchor bimetallic nanoparticles for EC−IRAS experiments, provides several key results. First, the Pt domain undergoes the slight electronic modification by the neighboring Ru. However, the degree of this modification is not significant enough to bring the catalytic activity changes, as also evident in the previous study showing that the surface Ru is mainly responsible for promoting CO electrooxidation.[9d,34] Second, the dipole coupling that obscures the analysis of EC−IRAS data for CO adlayers at saturation coverages should be considered, since there is "dipole coupling" between CO on Pt and Ru sites to a great extent. This complication can be minimized at lower coverages by "dosing" in the hydrogen region. Third, the two distinct CO bands on Pt and Ru islands were observed for the first time in nanometer-scale bimetallic systems; the individual CO components on Pt and Ru sites behave independently, electrooxidizing CO on Ru first, followed by CO on Pt with surface potential alterations. Also, it is shown that the electrooxidation of CO on large Ru islands is less facile than is the case on small Ru ones. Finally, the fact that a similar onset of CO oxidation on all Pt/Ru surfaces was found shows that the onset is governed by the presence of Pt/Ru boundaries and all Pt/Ru samples contain such boundaries.

Given the availability of well-developed strategies for preparing well-distributed nanoparticle films, together with the diversity of nanomaterials (monometallic and bimetallic systems with various size and compositions), we believe there are clearly tremendous opportunities for getting deep insight into the broad scope of catalytic reactions in controlled-potential (i.e., electrochemical) environments in conjunction with various spectroscopic means, as exemplified by the present study.

Acknowledgment. At Purdue, this work is supported by the grants from the National Science Foundation (Analytical and Surface Chemistry Program) and the Monsanto-Pharmacia Corp. via the Purdue Chemistry Industrial Associate Programs. At Illinois, this work is supported by the National Science Foundation Grant CHE-9985837 and by the U.S. Department of Energy, Division of Materials Sciences under Award No. DEFG02-91ER45439, through the FS-MRL at the University of Illinois at Urbana-Champaign.

JA028154X